# A Fast Ship Detection Algorithm Based on Automatic Censoring for Multiple Target Situations in SAR Images

Faical Farah, Toufik Laroussi and Hicham Madjidi



May 5, 2022

# A Fast Ship Detection Algorithm based on Automatic Censoring for Multiple Target Situations in SAR Images

Faiçal Farah
*Département d'Electronique, Laboratoire Signaux et Systèmes de Communication, 'SISCOM, Université des Frères Mentouri,*
Constantine, Algeria,
faicelfrh@gmail.com

Toufik Laroussi
*Département d'Electronique, Laboratoire Signaux et Systèmes de Communication, 'SISCOM, Université des Frères Mentouri,*
Constantine, Algeria,
toufik_laroussi@yahoo.fr

Hicham Madjidi
*Département d'Electronique, Laboratoire Signaux et Systèmes de Communication, 'SISCOM, Université des Frères Mentouri,*
Constantine, Algeria,
hichamfcm1279@gmail.com

*Abstract*—**Ship detection in multi-target Situations has become one of the crucial tasks in maritime surveillance. However, due to the existence of multiple Ship targets with different sizes in seacoast, standard Constant False Alarm Rate (CFAR) detection with a fixed guard window suffers from interfering targets within the training window. As a result, the probability of detection drops drastically. In this paper, a modified fast CFAR detection algorithm based on target indexing in multi-target situations is proposed. The detector does not require any guard window to prevent target interferences in the training window. It consists only of a training window and a test cell. It uses a novel interfering target-indexing matrix based on a maximally stable extremal region (MSER) detector that provides the training window with the interference pixels locations to be censored. The Generalized Gamma distribution (GΓD) is adopted as the statistical model of sea clutter. Experimental results show that the proposed method could achieve effective detection results of ships in multi-target situations compared to CFAR detectors with fixed guard window size.**

***Keywords—Ship Detection, CFAR algorithm, Automatic Censoring, Multi Target Situation, SAR Images.***

## I. INTRODUCTION

To overcome the coverage limitations of coastal systems, in nowadays, Synthetic aperture radar (SAR) images are widely used for maritime surveillance, where Ship detection and monitoring have become one of the most important applications in both civil and defense regimes. There are several strategies for ship target detection reported in the literature. One of the main algorithms that are exhaustively studied and applied in this field is the constant false alarm rate (CFAR) detection Strategy [1]. That is, each pixel from the SAR image is compared to an adaptive threshold calculated from the surrounding pixels located in the CFAR sliding window while maintaining constant the design false alarm probability. Note that the performance of such strategy depends strongly on various factors, namely, the statistical model of the local clutter, the sliding window dimensions which, in turn, is highly related to the estimated ship targets size, and the last but not least factor is the existence of multiple targets in a small area such as coastal zones [2].

The most frequently used CFAR detectors encountered in the literature include the Cell Averaging (CA-CFAR) detector, the Greatest of CFAR, the Smallest of CFAR, and the Order Statics CFAR. Unfortunately, each of them has its limitations [3-5]. In other words, there is no single detector performs well in all kinds of clutter backgrounds.

Basically, the CFAR detectors mentioned above work well in single target situations when a single ship exists in a locally Gaussian background. However, when using sliding windows to estimate local statistical parameters of the background clutter, there is a common problem of CFAR detectors that happens when multiple targets exist in the reference cells, which results in an overestimation of the adaptive threshold. Consequently, a drastic degradation in the detection performance is observed. To overcome this problem, various strategies have focused on censoring the interfering targets from the training window prior to any estimation of the statistical distribution parameters [6-8].

Based on the idea that the tailed part of the SAR image histogram represents the target class, an adaptive and fast (CFAR) algorithm based on automatic censoring is proposed by Gao *et al* [6]. In this method, an empirical parameter called censoring depth has to be set *a priori* based on a matrix index obtained by global thresholding of the input SAR image. An iterative censoring scheme (ICS) that updates the outliers for target detection is proposed by Cui *et al* [7]. Three years later, An *et al* [8] improved the ICS detector by, first censoring out both target and their neighborhood pixels present in the reference cells prior to the estimation of the parameters, and second, by adding a new initial detector to improve the convergence speed of the ICS detector.

For multiple target situations J. Ai et al [9], proposed a truncated clutter statistics-based joint-CFAR detector (TCSJ-CFAR) integrated with a CNN discriminator and an SVM classifier. The proposed method achieves a high prescreening rate and a better discrimination performance. In [10], a new Fast CFAR algorithm based on the density- censoring operation has been proposed to speed up the existing super-pixel (SP)-based CFAR detectors for ship detection in SAR images. The new CFAR algorithm shows a great computational improvement and leads to a more accurate adaptive threshold decision.

However, all previous works use a conventional CFAR stencil which consists of three regions; namely, the test cell, the guard region and the training region. One of the common situations is when the ship target to be detected is on a large scale. In this case, the guard region should be the size of the ship target. This makes the window larger and makes it contain multiple targets in the same position; which leads to an overestimation of the clutter model parameters.

In this paper, a new CFAR algorithm for ship detection in SAR images based on an accurate candidates extraction method and a new technique for target returns censoring is proposed. This has the effect of speeding up the detection process and suppressing the interfering ship targets. The detector consists only of a training region and a test cell. It uses a novel interfering target-indexing matrix based on an MSER detector that provides the training window along with the interfering pixels locations to be censored.

The paper is organized as follows. In Section 2, principles of the CFAR algorithm are given along with their limitations in real-world applications. In Section 3 the workflow of the proposed algorithm is presented to overcome the multi-target situations inherent in ship detection. In Section 4, experimental results are given with a detailed analysis. Finally, Section 5 concludes the paper.

## II. Principles of CFAR Detection

Given an image, and under the perfect scenario, which states that the background statistical model follows a Gaussian law, the aim is the detection of ship targets based on the characteristics of both classes "*targets*" and "*clutter*".

As shown in Fig. 1, the conventional CFAR sliding window is composed of three principal regions; namely, a test cell, a guard window, and a training window also called reference window.

The sliding window in a SAR image, the detector searches for target pixel values, which are unusually bright, compared to those in the neighborhood area, based on an adaptive threshold obtained from the reference cells in the sliding window and derived according to a given $P_{FA}$. Each test pixel is then compared to the obtained threshold to determine whether or not the pixel under test (PUT) corresponds to the targets class.

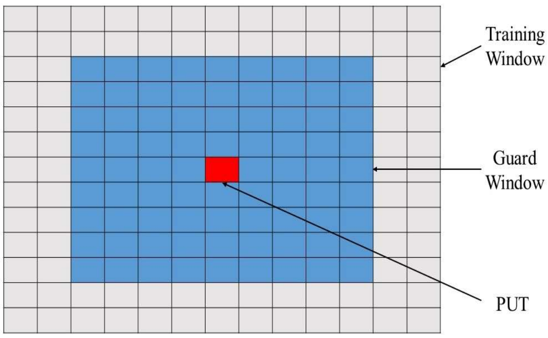


Fig. 1. Sliding Window in CFAR detection

Unfortunately, in real-word applications, the perfect scenario dimensioned above does not exist. In fact, many weather factors severely affect the sea state. As a result, the sea clutter statistical model could not allow a correct description of the backscattering signals. Moreover, since ship targets are not far enough from each other, this causes congestion, especially in the onshore areas. These multi-target situations affect the CFAR detection performance due to the presence of interferences in the detector region, dedicated to parameter estimation and threshold calculation. To overcome these two major problems, we, next, detail the workflow of the proposed algorithm.

## III. Workflow of the Proposed Algorithm

As the Generalized Gamma distribution (GΓD) has been shown to be an effective goodness of fit to the sea clutter, we choose it to describe the statistical model of such a type of clutter. In doing this, we present a new censoring algorithm based on an indexing map obtained by using the well-known maximally stable extremal region MSER detector [11], to eliminate the presence of any kind of interfering targets such as the ship positive interferences or the true negative interferences inherent to the man-made objects.

### *A. Statistical Modeling of Sea Clutter*

The $G\Gamma D$ has been used in the literature for ship target detection in SAR images [12]. It showed its ability to describe precisely the sea clutter. Its probability density function is given by [13].

$$p_X(x) = \frac{|\alpha|\beta^{\beta}}{\gamma\Gamma(\beta)} \left(\frac{x}{\gamma}\right)^{\alpha\beta-1} \exp\left\{-\beta\left(\frac{x}{\gamma}\right)^{\alpha}\right\}; \alpha, \beta, \gamma>0 \quad (1)$$

where, $\alpha$, $\beta$ and $\gamma$ refer to the scale, power, and shape parameters, respectively. Moreover, its estimators is obtained using the method of log-cumulants (MoLC).

For the observed data set of $N_C$ samples, which is denoted by $Z = \{Z_1, Z_2, Z_3, \dots, Z_{N_C}\}$, the first three empirical log-cumulants are computed as:

$$C_1 = \left(\frac{1}{N_C}\right) \sum_{i=1}^{N_C} \ln Z_i \quad (2)$$

$$C_2 = \left(\frac{1}{N_C}\right) \sum_{i=1}^{N_C} \ln(Z_i - C_1)^2 \quad (3)$$

$$C_3 = \left(\frac{1}{N_C}\right) \sum_{i=1}^{N_C} \ln(Z_i - C_1)^3 \quad (4)$$

According to (2)-(4) $\alpha$, $\beta$ and $\gamma$ are estimated by [10]:

$$\beta = \frac{\frac{C_2^3}{C_3^2} + \sqrt{\left(\frac{C_2^3}{C_3^2}\right)^2 + 2\left(\frac{C_2^3}{C_3^2}\right)}}{2} \quad (5)$$

$$\alpha = sgn(-C_3)\sqrt{\Psi(1,\beta)/C_2} \quad (6)$$

$$\gamma = \exp\{C_1 - (\Psi(\beta) - \ln(\beta)/\alpha\} \quad (7)$$

Where $sgn(.)$,$\Psi(x)$ and $\Psi(n,x)$ are the sign function, the digamma function and the *n*th-order polygamma function, respectively.

The GΓD is a versatile model that has many well-known clutter distributions including; the exponential, the Rayleigh, the Weibull, and the Gamma and its inverse as special cases. Let $F_X(x)$ be the cumulative distribution function (CDF). Then, for a given $P_{FA}$, the normalized threshold T *for* a *GΓD* background *can be shown to be as* [10].

$$T = \begin{cases} \gamma\left\{\frac{1}{\beta} Q_{Inv}(1 - P_{FA}, \beta)\right\}^{1/\alpha} & ,\alpha > 0 \\ \gamma\left\{\frac{1}{\beta} Q_{Inv}(P_{FA}, \beta)\right\}^{1/\alpha} & ,\alpha < 0 \end{cases} \quad (8)$$

where $Q_{Inv}(.,.)$ denotes the inverse incomplete gamma function.

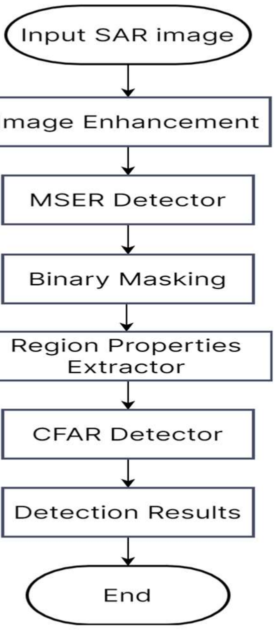


Fig. 2. Flow diagram of the proposed region proposal method.

Fig. 2 illustrates the detection workflow of the proposed algorithm. It includes ship candidates extraction and indexing, interference censoring, threshold calculation, and detection decision. The steps of the new method are as follows:

First of all, the process begins with smoothing-sharpening filter (SSF) [14], applied to the grayscale input SAR image to reduce the speckle noise effect and improve SAR image clarity. For instance, Fig. 3a shows an example of a 3D SAR image of a ship target, which has been passed through, a smoothing-sharpening filter, Fig 3b. We can clearly see the effect of this filter on the SAR image, in which the speckle noise is reduced with an edge awareness capability.

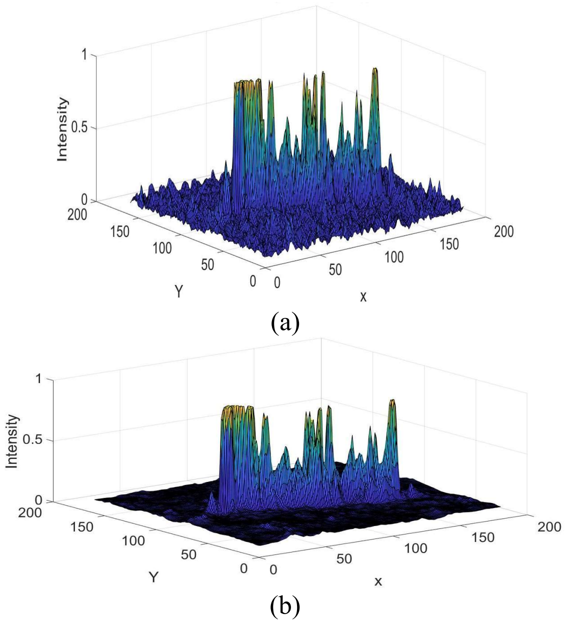


Fig. 3. (a) Three-Dimensional SAR image detail of ship target. (b) Effect of smoothing-sharpening Filter on the original SAR image.

Next, an MSER detector is applied to the smoothed grayscale SAR image to retrieve the object regions which are described by the pixel lists stored inside the returned regions object. An empirical parameter called the threshold delta is used to control the number of regions obtained by the detector. Then, a binary mask is applied to the output of the MSER detector by labeling the image into two classes, i.e, ‘1’ for objects and ‘0’ for background Clutter. Assuming a categorical image I, the region proprieties method returns measurements for the set of properties such as bounding boxes, centroid, area, etc. [15].

The bounding boxes extracted from the region proprieties method are used to automatically extract the ship candidate region from the input SAR image and their indexed matrix obtained by the MSER detector. Each proposed region has an index matrix of the object pixels coordinates. Only then, a GΓ-based CFAR detector is applied to each ship candidate's region using a sliding window without a guard window.

Fig. 4 illustrates the process of the proposed censoring method. The yellow and gray cells in Figs. 4a-b, describe, respectively, the interfering ship cells and the training cells without the interfering ship target ones. For each position $(X_n, Y_n)$ in a given candidate's region, the training window is multiplied by the ‘NOR’ version of the index matrix within the same position, Fig. 4-d. As a result, the set of clutter pixels is multiplied by ‘1’ and the object pixels are multiplied by ‘0’.

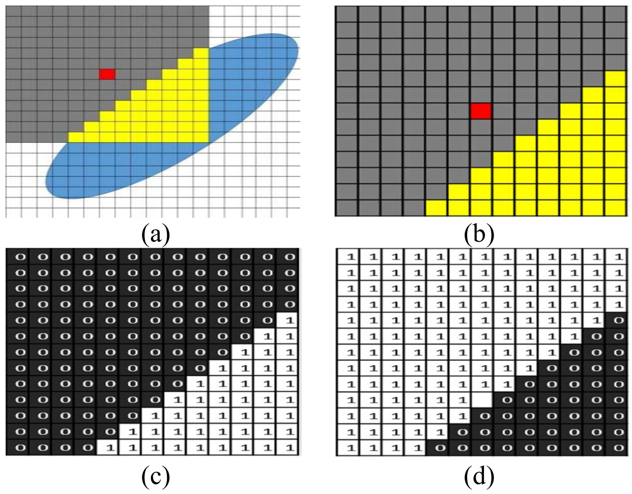


Fig. 4. (a) Demonstration of sliding window CFAR detector within a ship target region (b) Training window containing interfering ship target pixels. (c) Index matrix. (d) NOR version of the Index matrix.

Finally, the training cells are used for parameters estimation and the pixels values equal to ‘0’ are censored automatically. Note that by not using the default sliding window structure, we can use a larger number of training cells to estimate the statistical model parameters. This would result in the best adaptive threshold value, and consequently to the best detection. In addition, the CFAR detector has prior knowledge about the location of each object pixel that will be censored later using the coordinates of the object pixels list that extracted from the index matrix obtained by the MSER detector.

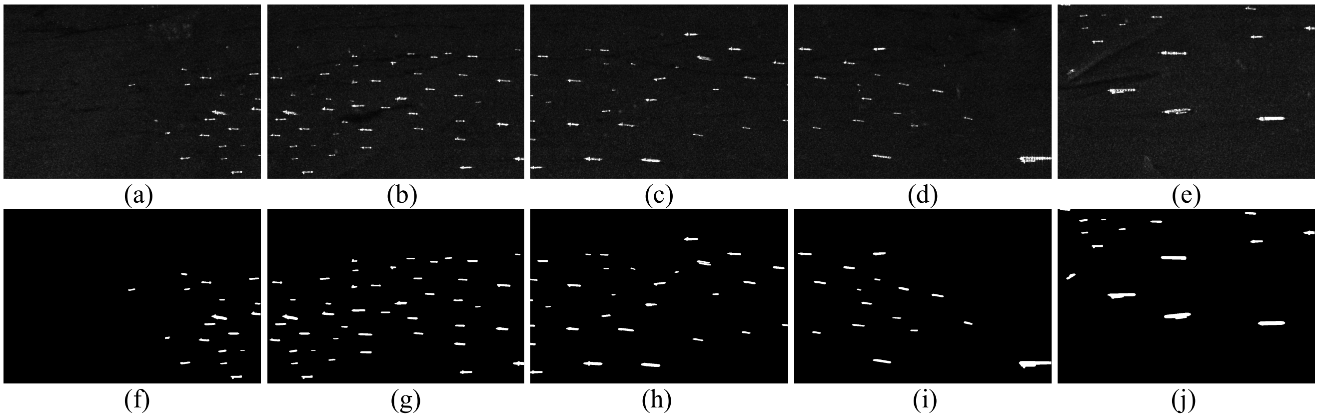


Fig. 5. (a)-(e) Original SAR images containing ship targets. (f)-(j) Their corresponding ground truth images.

## IV. Experimental results

To verify the effectiveness of the new censoring method, four 800 x 800 high-resolution (HR) SAR images are used for the test. All experiments are carried out on an i5 Dual-Core PC of 2.3 GHz processor and 8 GB of memory.

### *A. Dataset Description*

The dataset used for the performance assessment is composed of four HR Sentinel-1-B SAR images extracted from the HRSID Dataset [16], acquired by Strip Map acquisition mode of resolution 1.7m-3.6m in the range direction and 4.3m- 4.9m in the azimuth direction. The tested SAR images are acquired in both offshore and onshore areas where a wide variety of ships is presented in a small region. Furthermore, the ground truth images are available to validate the detection results.

### *B. Detection Results*

To present the efficiency of the proposed new method in terms of detection probability ($P_D$) and execution time, we compare quantitatively the performances of the new fast censoring algorithm, the improved two parameter CFAR detector [17], and the conventional CFAR detector based on the GΓD [12].
The Figure of Merit (FoM) is used to assess the $P_D$ of the three methods [18].

$$\mathrm{FoM} = \frac{N_{dt}}{N_{gt}+N_{fd}} \tag{3}$$

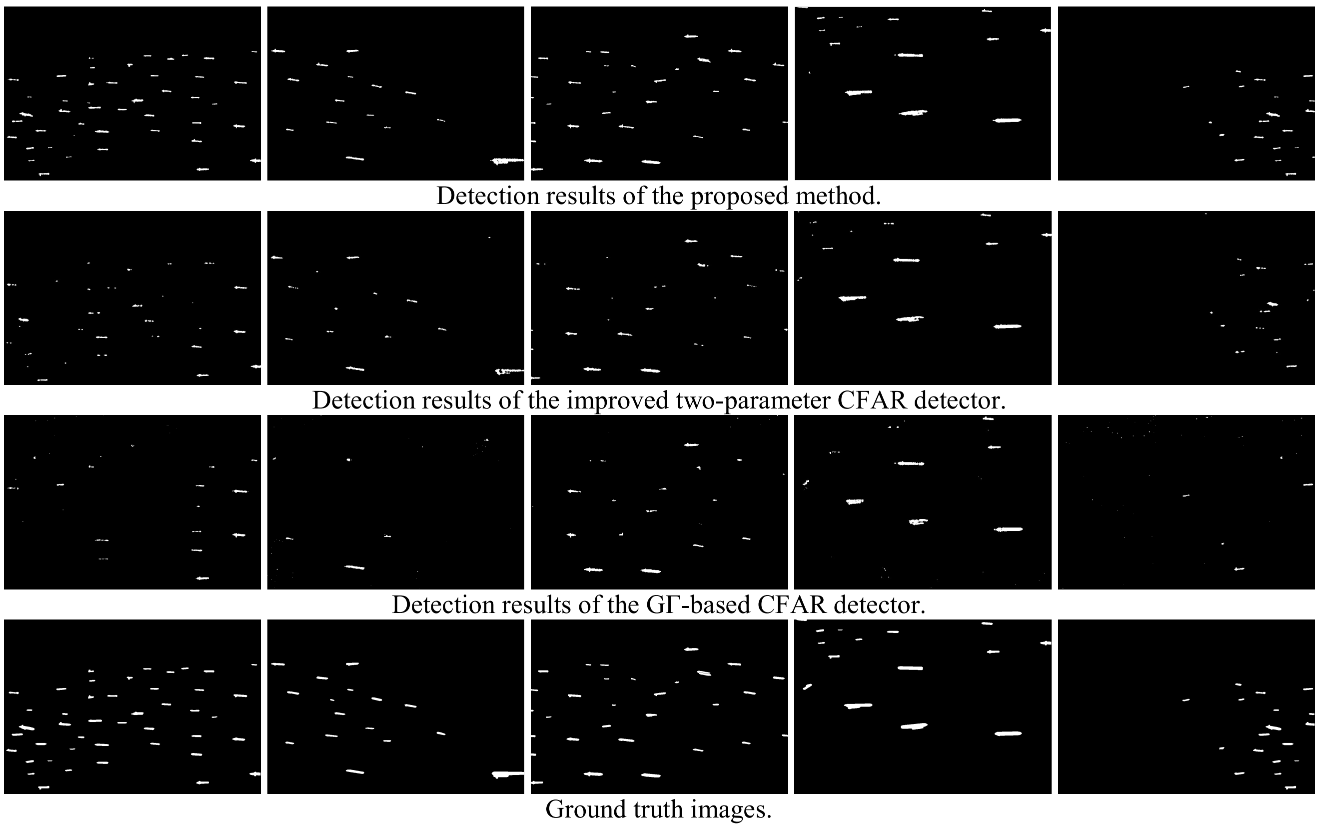


Fig. 6. Fig. 6. Detection results of the three detectors. First line: detection results of proposed method. Second line: detection results of the improved two-parameter CFAR detector. Third line: detection results of the GΓ-based CFAR detector. Fourth line: ground truth images.

Where $N_{dt}$, $N_{gt}$ and $N_{fd}$ are, respectively, the number of detected targets, the number of ground truth targets and the number of false detected targets. For all experiments, we set $P_{FA}$ =$10^{-5}$ as the design value.

As shown in Fig. 6, we can see that the improved two parameters CFAR detector produces high detection results and low false alarm rate compared to the standard GΓ-based CFAR detector which induces considerable number of false alarms and missing targets. However, the proposed algorithm outperforms both detectors with only a 2.4% FAR from 122 ships and achieves a higher accuracy rate of 97.6%.

**Table. I.** Detection performance comparison of the new automatic censoring algorithm and the GΓ-based CFAR detector on test images of Fig. 5.

| Performances | | Subsets | | | | |
|---|---|---|---|---|---|---|
| | | (a) | (b) | (c) | (d) | (e) |
| **Proposed Method** | $N_{gt}$ | 15 | 18 | 44 | 30 | 15 |
| | $N_{dt}$ | 15 | 18 | 44 | 30 | 14 |
| | $N_{fd}$ | 0 | 2 | 1 | 0 | 0 |
| | **FoM** | 1 | 0.9 | 0.97 | 1 | 0.93 |
| | **Running time (s)** | 13.25 | 5.526 | 11.187 | 9.842 | 6.915 |
| **Improved two-parameter CFAR detector** | $N_{dt}$ | 13 | 15 | 43 | 27 | 14 |
| | $N_{fd}$ | 0 | 3 | 1 | 1 | 1 |
| | **FoM** | 0.86 | 0.71 | 0.95 | 0.87 | 0.87 |
| | **Running time (s)** | 47.58 | 50.07 | 46.55 | 45.51 | 48.02 |
| **Generalized Gamma CFAR detector** | $N_{dt}$ | 9 | 4 | 15 | 15 | 5 |
| | $N_{fd}$ | 0 | 3 | 1 | 1 | 1 |
| | **FoM** | 0.32 | 0.16 | 0.28 | 0 .42 | 0.12 |
| | **Running time (s)** | 2861 | 1964.35 | 2239.82 | 2703.79 | 4049.78 |

In addition, as shown in Table I, the new fast detection algorithm produce higher FoMs and smaller running times than the reference methods [12], [17].

To assess the detection results of previous detectors, we draw the Receiver Operating Characteristic (ROC) curves in terms of FOM and $P_{FA}$.

As shown in Fig. 7, the ROC curves of the three detectors indicate that the proposed algorithm perform better than the improved two-parameters CFAR detector and exhibits much better performance than the conventional GΓ-based CFAR detector.

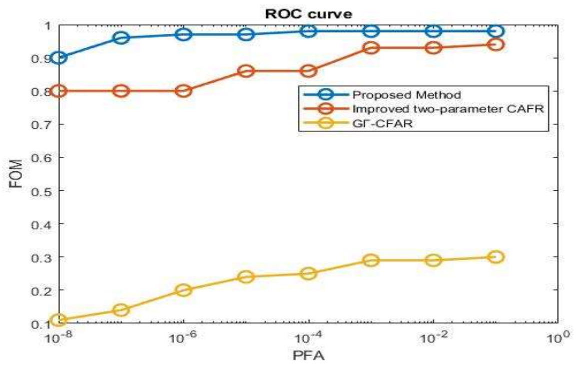


Fig. 7. ROC curves of the three detectors.

When PFA is as low as $10^{-8}$, the FOM of the proposed algorithm is about 0.1 higher than the improved two-parameter CFAR detector and about 0.79 higher than the conventional GΓ-based CFAR detector. When $P_{FA}$ increases to $10^{-5}$, the FOM of our proposed algorithm is 0.13 higher than the two-parameter CFAR detector. Finally, when $P_{FA}$ increases to $10^{-1}$ , the FOM of the proposed algorithm is 0.04 higher than the two-parameter CFAR detector and about 0.68 higher than the conventional GΓ-based CFAR detector. Another interesting remark can be deduced from the ROC curves. That is when the $P_{FA}$ decreases to $10^{-8}$, the proposed method has a slight change in FOM value compared to the existing ones. This shows the capability of the new algorithm to handle the multi-target situations.

Since real-time applications such as maritime surveillance, need a very low time response that cannot be achieved even with the use of the proposed algorithm, we conclude that it could be used with the recent deep learning object detection networks to yield more accurate results.

## V. Conclusion

In this paper, a fast CFAR algorithm based on automatic censoring method for ship target detection in SAR images is proposed. In achieving this, we first pass a grayscale SAR image through a SSF in order to reduce the speckle noise effect and improve its quality. Next, we apply the MSER detector to generate an index matrix, and a set of proposal regions are extracted from the obtained index matrix. Then, a GΓ-based CFAR detector is applied to each ship candidate's region to detect the true ship targets. Finally, the hypothesis test is obtained via the comparison of each gray level with the adaptive threshold. Experimental Results on the tested SAR images reveal that, the proposed fast ship detection algorithm based on automatic censoring outperforms the two-parameter CFAR detector and the GΓ-based adaptive CFAR detector in detection performances and running time as well. In the future, the proposed method will be tested on more real SAR images to verify its effectiveness.

## References


[1] D. J. Crisp, "The state-of-the-art in ship deteciton in synthetic aperture radar imagery," Intellegence, Surveillance and Reconnaissance Division Information Sciences Laboratory, Defense Science and Technology Organization, Department of Defense, Australian Government, DSTO-RR-0272 (2004).

[2] H. Rohling, "Radar CFAR thresholding in clutter and multiple-target situations", IEEE Trans. Aerosp. Electron. Syst., vol. AES-19, pp. 608-621, July 1983.

[3] K. El-Darymli, P. McGuire, D Power, C. Moloney, "Target detection in synthetic aperture radar imagery: A state-of-the-art survey", *J. Appl. Remote Sens*, Vol. 7, No. 1 pp. 071598, 2013.

[4] [4] D. J. Crisp, "The state-of-the-art in ship detection in synthetic aperture radar imagery,'' DSTO Information Sciences Laboratory, Edinburgh, Australia, Tech. Rep. RR-0272, May 2004.

[5] [5] C. Oliver and S. Quegan, *Understanding Synthetic Aperture Radar Images*. Raleigh, NC, USA: Scitech, 2004.

[6] G. Gao, L. Liu, L. Zhao, G. Shi, and G. Kuang, "An adaptive and fast CFAR algorithm based on automatic censoring for target detection in high-resolution SAR images," *IEEE Trans. Geosci. Remote Sens.*, vol. 47, no. 6, pp. 1685–1697, Jun. 2009.

[7] Y. Cui, G. Zhou, J. Yang, and Y. Yamaguchi, "On the iterative censoring for target detection in SAR images," *IEEE Geosci. Remote Sens. Lett.*, vol. 8, no. 4, pp. 641–645, Jul. 2011.

[8] W. An, C. Xie and X. Yuan, "An improved iterative censoring scheme for CFAR ship detection with SAR imagery", IEEE Transactions on Geoscience and Remote Sensing, vol. 52, no. 8, pp. 4585-4595, 2014.

[9] J. Ai, R. Tian, Q. Luo, J. Jin, and B. Tang, ‘‘Multi-scale rotationinvariant Haar-like feature integrated CNN-based ship detection algorithm of multiple-target environment in SAR imagery,’’ IEEE Trans. Geosci. Remote Sens., vol. 57, no. 12, pp. 10070–10087, Dec. 2019.

[10] X. Wang, G. Li, X. -P. Zhang and Y. He, ”A Fast CFAR Algorithm Based on Density-Censoring Operation for Ship Detection in SAR Images,” in IEEE Signal Processing Letters, vol. 28, pp. 1085-1089, 2021.

[11] Nister, D., and H. Stewenius, "Linear Time Maximally Stable Extremal Regions", Lecture Notes in Computer Science. 10th European Conference on Computer Vision, Marseille, France: 2008, no. 5303, pp. 183–196.

[12] X. Qin, S. Zhou, H. Zou, G. Gao, “A CFAR Detection Algorithm for Generalized Gamma Distributed Background in High Resolution SAR Images, IEEE Geosci. Remote Sens. Lett, Vol 10, No. 10, pp. 806-810, 2013.

[13] H. C. Li, W. Hong, Y. R. Wu, and P. Z. Fan, “On the empirical statistical modeling of SAR images with generalized gamma distribution,” *IEEE J. Sel. Top. Signal Process*., Vol. 5, No. 3, pp. 386-397, Jun 2011.

[14] G. Deng, F. Galetto, M. Al-Nasrawi and W. Waheed, "A guided edge-aware smoothing-sharpening filter based on patch interpolation model and generalized gamma distribution", IEEE Open J. Signal Process., vol. 2, pp. 119-135, 2021.

[15] Demirkaya, O., Asyali, M.H., & Sahoo, P.K. (2009). Image Processing with MATLAB: Applications in Medicine and Biology. CRC Press. https://doi.org/10.1201/9781420008937

[16] S. Wei, X. Zeng, Q. Qu, M. Wang, H. Su and J. Shi, "HRSID: A High-Resolution SAR Images Dataset for Ship Detection and Instance Segmentation", IEEE Access, vol. 8, pp. 120234-120254, 2020.

[17] R. Wu, ‘’ Two-Parameter CFAR Ship Detection Algorithm Based on Rayleigh Distribution in SAR Images’’, Preprints 2021, 2021120280 (doi: 10.20944/preprints202112.0280.v1).

[18] C. Chen, X. Li,” A new CFAR algorithm based on variable window for ship detection in SAR images”, Signal Image Video Prosses, Vol. 13, No. 4, pp. 779-786, 2019.